WORLD CONFERENCE ON TIMBER ENGINEERING 2025
BRISBANE, AUSTRALIA
Advancing Timber for the Future Built Environment

Response of Mass Ply Panel, Self-centering Rocking Walls with Buckling-Restrained Boundary Elements as Energy Dissipators in Shake Table Testing

Morgan McBain[1], Ludovica Pieroni[2], Gustavo A. Araújo R.[3], Barbara G. Simpson[4], Andre R. Barbosa[5], John W. van de Lindt[6], Arijit Sinha[7], Steven Kontra[8], Prashanna Mishra[9], Steve Pryor[10], Patricio A. Uarac P.[11], Tanner J. Field[12]

ABSTRACT: A full-scale, six-story, mass timber building including Mass Ply Panel (MPP) self-centering rocking walls with Buckling-Restrained Boundary Elements (BRBs) was tested at the Large High-Performance Outdoor Shake Table (LHPOST6) at the University of California, San Diego (UCSD). Measured sensor and derived data included global responses, such as floor displacements and accelerations, along with local responses, such as post-tensioning (PT) forces and uplift displacements, among others. The three-dimensional shake table testing program included 23 ground motion records with intensities of shaking ranging from Service (SLE) up to Risk-Targeted Maximum Considered Earthquake (MCE_R) levels. Results highlighted that: [i] the drift response was near uniform along the height of the building, [ii] the acceleration response included large contributions from the higher modes, [iii] the PT rods remained elastic and had stable post-tensioning force throughout the test program, and [iv] the self-centering system resulted in negligible residual drifts. Qualitative observations from construction and testing were also cataloged to further support the feasibility of implementation in practice. By combining steel BRBs and post-tensioning rods with MPP rocking elements, the system was able to meet the enhanced seismic performance goals targeted for the project. Future work will seek to define both resilience and sustainability targets for designs incorporating multiple performance objectives.

KEYWORDS: Hybrid Lateral System, Low-damage, Mass Timber, Rocking Wall, Shake Table

[1] McBain, Civil and Environmental Engineering, Stanford University, Stanford, CA, USA, mmcbain@stanford.edu
[2] Pieroni, Civil, Environmental, and Geomatic Engineering, University College London, London, UK, ludovica.pieroni.20@ucl.ac.uk
[3] Araújo R., Civil and Environmental Engineering, Stanford University, Stanford, CA, USA, garaujor@stanford.edu
[4] Simpson, Civil and Environmental Engineering, Stanford University, Stanford, CA, USA, bsimpson@stanford.edu
[5] Barbosa, Civil and Construction Engineering, Oregon State University, Corvallis, OR, USA, andre.barbosa@oregonstate.edu
[6] van de Lindt, Civil and Environmental Engineering, Colorado State University, Fort Collins, CO, USA, jwv@colostate.edu
[7] Sinha, Wood Science & Engineering, Oregon State University, Corvallis, USA, arijit.sinha@oregonstate.edu
[8] Kontra, Civil and Construction Engineering, Oregon State University, Corvallis, OR, USA, steven.kontra@oregonstate.edu
[9] Mishra, Civil and Environmental Engineering, Colorado State University, Fort Collins, CO, USA, prashanna.mishra@colostate.edu
[10] Pryor, Research & Development, Simpson Strong-Tie, Pleasanton, California, United States, spryor@strongtie.com
[11] Uarac P., Civil and Construction Engineering, Oregon State University, Corvallis, OR, USA, uaracpip@oregonstate.edu
[12] Field, Civil and Construction Engineering, Oregon State University, Corvallis, OR, USA, tanner.field@oregonstate.edu

https://doi.org/10.52202/080513-0300

1 – INTRODUCTION

To target both sustainability and seismic resilience, the design of buildings needs to be customized to meet targeted objectives able to account for multiple performance metrics. By combining the stable energy dissipation properties of steel with the environmental and aesthetic advantages of engineered wood, mass timber self-centering rocking walls with buckling-restrained boundary elements represent a potential mixing-and-matching of materials and devices to begin to target tailored sustainable and seismic performance goals [1-3]. Since the seismic design of mass timber is only beginning to be codified, the use of recognized energy dissipators such as BRBs lowers barriers to less well-established lateral-force resisting systems (LFRS).

The primary component of the proposed LFRS is full-height mass timber panels designed to remain essentially elastic at high levels of shaking to enforce a global tilting mode, effectively mitigating the formation of story mechanisms [4]. Sacrificial energy dissipation elements and self-centering mechanisms may also be included to enhance performance. To date, researchers have conducted experimental investigations of mass timber rocking walls with a variety of distributed or concentrated energy dissipators along with PT [5-14].

In the literature, LFRS combining mass timber with steel BRBs have been designed and tested [15-18]. Most notably, Araújo et al. [17-18] conducted quasi-static testing of a three-story mass timber wall with vertically oriented BRBs at the base. Rather than uplifting, the wall "pivoted" about a pinned base without a self-centering mechanism. The LFRS was found to distribute drift demands along the height of the building, effectively mitigating story mechanisms that can induce costly damage. Additionally, the BRBs were able to sustain high displacement demands with full and stable energy dissipation capacity. However, since the system tended to unload based on the initial stiffness of the BRBs, the LFRS exhibited residual drifts upon completion of the testing that may exceed repairability limits. Moreover, the testing was conducted quasi-statically and did not include the influence of dynamic effects.

The inclusion of post-tensioning rods to aid in self-centering the system could increase functionality after a seismic event. This study builds upon the existing literature by: (1) conducting experimental testing of a self-centering mass timber rocking wall with BRBs and post-tensioning; (2) generating an extensive set of dynamic shake-table test data, which can be used in future studies; and (3) cataloging the construction process of the LFRS to inform future installations.

A full-scale, six-story mass timber building with Mass-Ply Panel (MPP) self-centering rocking walls and BRBs (MPP-BRB walls) was tested at the NHERI @ UCSD LHPOST6 facility in January 2024. Each MPP-BRB wall was equipped with two BRBs oriented vertically at the base and four post-tensioning rods that extended from the base to the top of wall. Base resisting moment was provided primarily by the BRBs, which were connected to the wall near the base and bolted to a steel foundation made of beams attached to the shake table surface. The PT rods were designed to remain elastic beyond MCE_R demands, providing additional elastic restoring moment to enable re-centering of the building after each test. To balance the overturning moment from the BRBs and PT and more easily enforce a global tilting mode, the walls were not directly anchored to the foundation but rather allowed to uplift and rock.

2 – PROJECT DESCRIPTION

This paper focuses on the second phase of the NHERI Converging Design project, which focused on the MPP-BRB walls [19]. The first phase of NHERI Converging Design tested self-centering mass timber rocking walls with u-shaped flexural plates (UFPs) for distributed energy dissipation [20]. The third phase studied the hybrid behavior of a seismically resilient steel frame with the mass timber gravity system [21].

The test specimen for the project was inherited from the NHERI TallWood team [14]; the top four stories of the TallWood ten-story specimen were deconstructed, and the original north-south (N-S) lateral system was replaced with the MPP-BRB walls. Additionally, non-structural facades present for the TallWood tests and first phase of the Converging Design project were removed.

2.1 TEST BUILDING

The test specimen was six stories tall and had a 10.46m x 10.51m floor plan with MPP-BRB walls in the N-S direction and cross laminated timber (CLT) self-centering rocking walls with UFPs as energy dissipators in the east-west (E-W) direction. The E-W direction LFRS was inherited from the first phase of Converging Design [20].

A view of the test building in place at the LHPOST6 is shown in Fig. 1. The first story height was 4.0m and upper stories had a typical story height of 3.4m.

The typical floor plan is shown in Fig. 2. The floor plan was symmetrical across the N-S central axis. In the opposite direction, the central stairwell and MPP-BRB rocking walls were staggered across the E-W centerline.

https://doi.org/10.52202/080513-0300

Figure 1: Test building from northeast corner

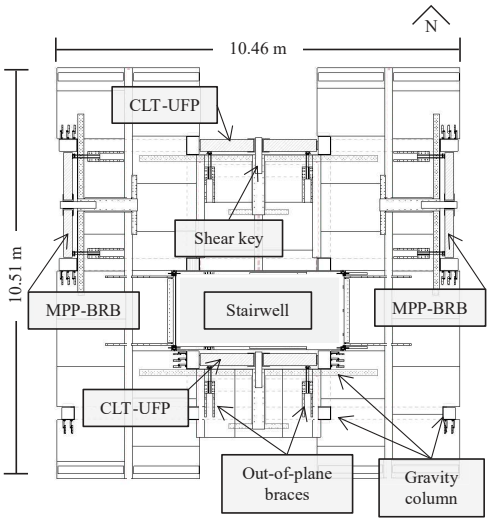

Figure 2: Test building typical floor plan

Lateral forces were transferred from the diaphragms to the walls using vertically slotted shear keys, which allow the wall to uplift and rock without constraint. Similarly, vertically-slotted braces provided out-of-plane stability but did not restrict the in-plane wall motion.

The gravity system for the test specimen was constructed with laminated veneer lumber (LVL) beams and columns [22], and the diaphragms were constructed with an array of timber products including CLT, glue-laminated timber (GLT), nail laminated timber (NLT), and dowel laminated timber (DLT) [23]. All columns were pinned at the base, and gravity connections had rotation capacity of 0.05 rad [24].

2.2 TESTING PROGRAM

A total of 23 shake table tests were run as part of the test program. Of these 23 tests, 18 made up the primary testing and the last five were conducted for an internal shake-table calibration study. The ground motions (GM) selected for testing ranged from intensities of $0.1\times MCE_R$ to $1.1\times MCE_R$ based on a hypothetical Seattle site and were representative of crustal, interface, and intraslab seismic events. The records were selected from the NGA-West2 [25] and NGA-Sub [26] databases, then individually scaled to match the MCE_R spectrum by minimizing the mean square error (MSE) over the period range of 0.22 seconds ($0.2\times T_1$) to 1.55 seconds ($1.5\times T_1$). The fundamental period T_1 is the first-mode period in the N-S direction estimated from a complementary numerical model.

A test matrix is provided in Table 1. Among the records, the Northridge-01 ground motion was chosen as a benchmark to isolate behavior in the N-S, E-W, and vertical directions. Based on the capacity of the shake table, the Maule, Chile record could only be run with bidirectional shaking for higher shaking intensities.

In addition to the shake table tests, low-amplitude white noise shakes were run independently in both the N-S and E-W directions to tune the controls for the shake table, estimate periods of the structure, and monitor for significant damage during testing. The white-noise amplitude was sufficiently high to initiate rocking, but not large enough to yield the BRBs.

https://doi.org/10.52202/080513-0300

Table 1: Summary of Testing Program

GM ID	GM Name	Direction*	MCE_R SF**	% MCE_R
1	Northridge-01	XYZ	1.58	10%
2	Northridge-01	Y	1.58	10%
3	Northridge-01	Y	1.58	30%
4	Northridge-01	XY	1.58	30%
5	Northridge-01	XYZ	1.58	30%
6	Northridge-01	Y	1.58	67%
7	Northridge-01	XYZ	1.58	67%
8	Northridge-01	XYZ	1.58	100%
9	Niigata, Japan	XYZ	1.32	30%
10	Ferndale 890	XYZ	4.53	30%
11	Maule, Chile	XYZ	1.54	30%
12	Ferndale 890	XYZ	4.53	67%
13	Maule, Chile	XY	1.54	67%
14	Niigata, Japan	XYZ	1.32	69%
15	Ferndale 890	XYZ	4.53	100%
16	Maule, Chile	XY	1.54	100%
17	Niigata, Japan	XYZ	1.32	100%
18	Northridge-01	XYZ	1.58	110%

*"X" refers to E-W, "Y" refers to N-S, and "Z" indicates vertical motion

**MCE_R SF refers to the scale factor on the raw ground motion record for the MCE_R intensity test.

3 – EXPERIMENTAL SETUP

The following sections provide details on the LFRS construction process, instrumentation scheme, and data processing methods.

3.1 CONSTRUCTION

The MPP-BRB LFRS was erected over a period of three weeks by five skilled laborers. Equipment used throughout the process included a crane, forklift, and boom lift. First, steel components such as the shear keys, wall armour, and connection plates were attached to the MPP panels on the ground and the BRB attachment was mocked-up (Fig. 3a). BRBs were connected to the MPP panel using a u-shaped steel saddle secured with 45-degree SDCF screws and MTW45 washers to create a strong, stiff, low-deformation connection, see Fig 4. Each wall consisted of two MPP panels spliced with a glued-in-rod connection [27]. As such, the second step was to prepare the pilot holes for the spliced connection. Once prepared, the walls tested during Phase 1 of Converging Design were removed and replaced one-by-one with the MPP-BRB walls; first the east wall, then the west. The lower wall panel was lifted with a crane and the BRBs were attached using a forklift (Fig. 3b). The panel was placed on the foundation with a crane; minor adjustments were made using the forklift as the wall was placed (Fig. 3c). Next, the second panel was placed (Fig. 3d) and connections were secured (epoxying splice, fastening out-of-plane braces, fastening BRBs to foundation). Finally, the PT rods were moved into position and post-tensioning forces were applied using a jack at the roof level. Note, due to contractor availability, the walls were erected before the non-structural facades were removed.

3.2 INSTRUMENTATION

Data were collected using approximately 600 sensors, consisting primarily of accelerometers, string potentiometers (SP), linear variable displacement transducers (LVDTs), and strain gauges (SG). The placement of instruments targeted both global behavior, such as floor acceleration and displacement, and local behavior, such as forces in the BRBs, stress in the post-tensioning rods, and wall uplift, among others. Floor accelerations were derived using two accelerometers at the center of mass of each floor – one which sampled at a frequency of 256 Hz, and one at 1000 Hz. Floor displacements were measured with two SPs per floor, which spanned from the floor diaphragms to fixed safety towers on the south side of the building. Vision-based measurements also provided complementary measurements of global displacements [28]. Forces in the PT rods were measured with two SG per rod. Both SP and SG had a sampling frequency of 256 Hz.

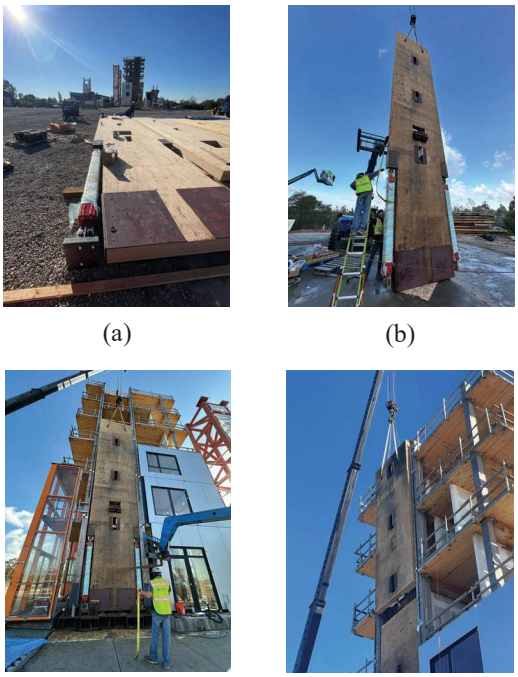

(a) (b) (c) (d)

Figure 3: Test building construction

3.3 DATA PROCESSING

Data processing procedures were informed upon review of the frequency content of the raw data records, eigenvalue analysis of a numerical model, and discussions with shake-table operators regarding suggested best practice. Baseline correction and band-pass filter cutoff frequencies were chosen based on a quantitative and qualitative study which identified the filter bounds that best match measured displacements when acceleration records are double integrated [19], [29]. The procedure for processing accelerometer records is summarized as follows:

1. Load raw acceleration record, and multiply by gravitational constant.
2. Baseline correct to remove linear trends.
3. For the 1000 Hz accelerometers, clean the record based on jerk observations:
   a. Identify points where the jerk is both double-ended and has an amplitude larger than 10% of the absolute maximum jerk.
   b. Remove and replace these points with the mean value of the two neighbouring points.

   This step resulted in filter distortion when applied to the 256 Hz accelerometers due to their lower sample rate (i.e. the detected double-ended jerks may be within the sample rate).
4. Add half-cosine tapers to both ends of the record.
5. Add zero padding to both ends of the record.
6. Apply a fourth-order Butterworth band-pass filter with low cutoff frequency of 0.1 Hz and high cutoff frequency of 50 Hz.
7. Remove zero padding from the record.

The same procedure was used for the SP data to identify peak story drifts, except for steps (3) and (4). Additionally, a low-pass Butterworth filter was applied rather than a band-pass filter. Records were processed on an individual basis (i.e. baseline corrected to be centered around zero for each test). The same applies for identifying maximum forces in the PT rods, except that the records were not baseline-corrected.

To preserve information, residual displacements and initial forces in the PT rods were determined through consideration of raw displacement records. Notably, the process described above has the potential to remove residual measurements as the low-pass Butterworth filter can cause some distortions at the beginning and end of the records. Thus, the residual displacement was taken as the difference between the mean value of the last 256 points (last one second) and the mean value of the first 256 points (first one second) of the raw displacement record. The residual drift was independently evaluated for each test, not accumulated. The initial force for the PT rods was taken as the average value of the first 30 points in the record for each test.

4 – RESULTS

The following sections summarize lessons learned during construction of the test building, measured structural response, and findings from on-site damage assessments. Additional information can be found in [19].

4.1 CONSTRUCTION LESSONS

To inform future designs, lessons learned during the construction process were documented:

1. BRBs should be oriented in a manner that supports ease of replacement after a seismic event. The orientation of the BRB gusset plates for the test building was such that they could not be installed or removed without complete removal of the columns or wall panels, as shown in Fig. 4. To fulfill their role as sacrificial, replaceable energy dissipation elements, the gussets can be oriented out-of-plane.
2. The MPP panels should be sized such that the splice occurs at a location easily accessible for continued work. The splice location for the test building walls was such that a raised platform needed to be used to finish the epoxy work. Lowering the splice to mid-height of the story would have accelerated construction and increased ease of installation.
3. The accuracy of post-tensioning procedures should be considered in the design. During the first phase of the Converging Design project, the procedure used to post-tension the rods on site was found to have a high chance of overshooting the target PT force. Following this observation, the target PT force for the MPP-BRB wall was lowered from that of the original design to ensure the PT bars did not exceed their yield strength. In the future, designers may benefit from considering a range of acceptable PT forces.
4. Special attention should be paid to wall-bounding elements to ensure the wall has space to rock, see Fig. 4. During construction, the team realized that steel backer plates remaining on the bounding gravity columns from the first phase of the Converging Design project were not initially considered during the design of the wall. As such, the wall panels had to be trimmed on-site to fit the space and be able to rock uninhibited.
5. The placement of structural elements with slotted connections should consider the expected uplift and compression of the wall. For example, the team worked closely with the contractor to ensure out-of-

https://doi.org/10.52202/080513-0300

plane braces with vertically slotted connections were placed such that bolts lied near the top one-third of the slot so they could move both up and down as the wall rocked, see Fig. 5. Initially, the contractor placed some bolts too high or low in the slot for the wall to be able to rock. The bolt placement had not been clearly detailed in the construction drawings.

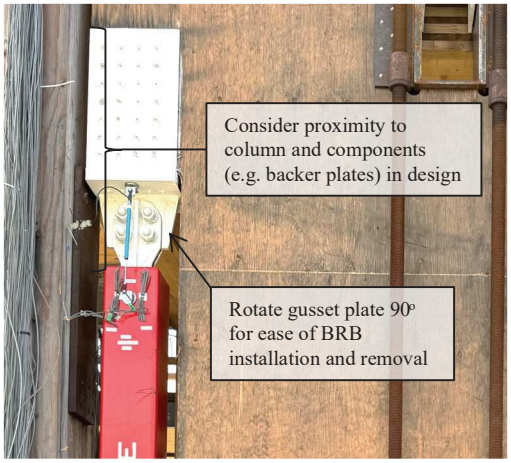

Figure 4: Construction considerations for wall design

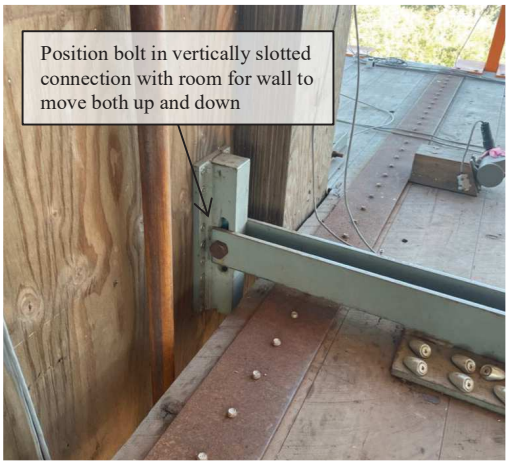

Figure 5: Construction consideration for vertically slotted connections, out-of-plane brace example from CLT-UFP wall

4.2 STRUCTURAL RESPONSE

Global (acceleration, drift) and local (PT force) responses are shown in Fig. 6-10. Discontinuous lines and missing markers in plots are representative of locations where a sensor was missing/damaged and deemed unreliable.

Fig. 6. shows the peak absolute floor accelerations and peak story drift ratios observed for the Northridge-01 sequence. The drift response was near uniform over the height of the building at all intensities, demonstrating that the MPP-BRB LFRS successfully enforced a global tilting displaced shape. In contrast, floor accelerations exhibited larger contributions from higher mode effects, especially as the shaking intensity increased and the BRBs yielded. While observed across all ground motions, this trend tended to be more significant for GMs with higher spectral content near the higher-mode periods, indicating that designers may want to consider higher-mode contributions for force- and acceleration-sensitive components.

Fig. 7 and Fig. 8 present the maxima of the peak absolute floor accelerations and story drift ratios observed throughout the testing program, respectively. That is, the figures show the maximum response observed across all floors for each test. A maximum peak absolute floor acceleration of 1.73g and maximum story drift ratio of 2.09% were observed at the $1.1\times MCE_R$ intensity level for the Northridge ground motion record. Story drift ratios were within intended limits established for testing: a maximum of 2% for the design earthquake (DE) and 3% for MCE_R.

Fig. 9 presents the average initial PT force per rod and the average maximum PT force per rod for each test. The PT rods did not yield and sustained a range of stable forces throughout the testing program, as indicated by the initial and maximum values. The system successfully re-centered after each ground motion. The results are presented for the east wall and west wall (both MPP-BRB) separately. Notably, there is an increase and decrease in initial PT force for the walls aligning with morning and afternoon testing blocks. While the SG had temperature compensation, the direct sun likely influenced the readings and the moisture content of the wall.

https://doi.org/10.52202/080513-0300

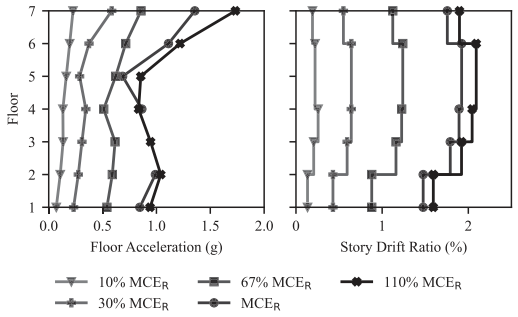

Figure 6: Northridge-01 sequence peak absolute floor accelerations and peak story drift ratios

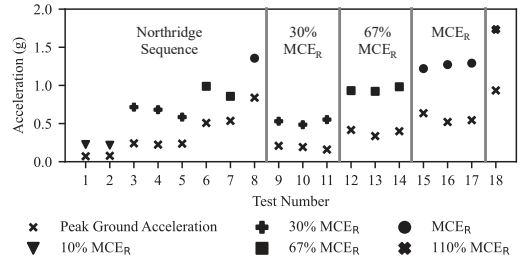

Figure 7: Maximum absolute floor accelerations

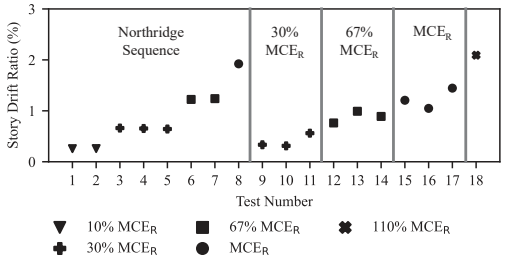

Figure 8: Maximum peak story drift ratios

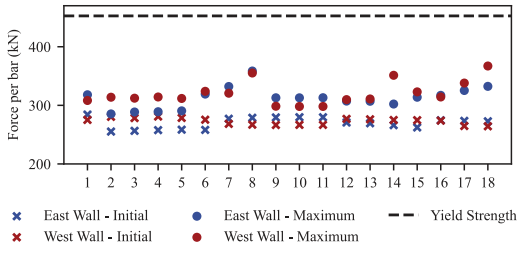

Figure 9: Initial and maximum PT rod forces

As shown in Fig. 10, a maximum residual story drift ratio of 0.16% was observed throughout the test program. While residual drifts are presented on a test-by-test basis, they notably did not accumulate. That is, the structure re-centered from test to test, and residual drifts did not accumulate in the building over time. The maximum residual story drift ratios observed were well below the typical constructability tolerance in the United States of 0.20% [30-31], indicating that the structural system would not require immediate repair for the shaking intensities considered. More information about acceleration-sensitive components, which were not part of the testing program, would also be needed to more fully assess loss.

5.3 DAMAGE OBSERVATIONS

Throughout the testing program, systemic damage inspections were performed. Key aspects of the structural system including BRBs, wall splices, out-of-plane braces, UFPs, base of the wall panels, and gravity connections were monitored. The wall splices, base of wall panels, and gravity connections remained in-tact with no visual damage observed throughout the testing program. The out-of-plane braces performed as intended and generally remained undamaged. However, some bolts of the braces were tightened two to three times throughout the testing program as they loosened during the series of shaking. The BRBs and UFPs both experienced inelastic deformations, as intended.

Images of the northeast BRB at key moments in the testing program are shown in Fig. 11. As the PT rods performed as expected, the permanent deformation in the BRBs did not affect the residual position of the building. The deformation also did not affect the ability of the BRBs to sustain continued shaking. In practice, the damaged BRBs would have fulfilled their role as sacrificial energy dissipators and could be removed and replaced after a seismic event.

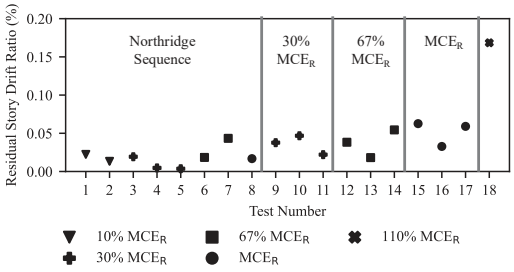

Figure 10: Maximum residual story drift ratios

https://doi.org/10.52202/080513-0300

(a) (b) (c)

Figure 11: Upper end of northeast BRB (a) before shaking, (b) after GM 7, and (c) after GM18

5 – CONCLUSION

A full-scale six-story building with mass timber, self-centering rocking walls using vertically oriented BRBs as concentrated energy dissipators was tested under 23 earthquake shake table tests. The construction process was cataloged to document lessons learned for future design and construction of LFRS using MPP-BRB walls. Measured and derived data along with damage inspections show that the structural system performed as expected. Specifically, the test building response under dynamic loading is summarized:

1. The MPP-BRB walls were shown to mitigate the formation of story mechanisms under dynamic loading. Most importantly, the drifts were evenly distributed along the height. Maximum peak story drift ratios of 1.24% and 1.92% were observed at the DE and MCE_R levels, respectively. These observed demands were within the targeted limits of 2% and 3% story drift ratio at DE and MCE_R.
2. Acceleration results suggest that higher-modes contributions could impact force- and acceleration-sensitive structural and non-structural components. A maximum peak absolute floor acceleration of 1.73g was observed at the $1.1\times MCE_R$ level. Floor accelerations had significant contributions from higher modes, especially at DE and greater intensities of shaking after the BRBs had yielded.
3. Residual drift data demonstrate that the self-centering MPP-BRB wall may enable immediate re-occupancy of a building after a large seismic event and that the structural system would not require immediate repair. The PT rods remained elastic throughout the testing program and effectively re-centered the structure. The test building experienced residual drift ratios well below the typical tolerance for new construction in the United States (0.2%). The maximum observed residual story drift ratio was 0.16% after the $1.1\times MCE_R$ level Northridge test.
4. Notable permanent damage to the structural system was limited to permanent elongation of the BRBs, which were designed as sacrificial energy-dissipation elements. The elongation of the BRBs did not affect the residual position of the test building. In future designs, the orientation of the BRBs should be considered for ease of removal and replacement.

For further information beyond this paper, an extensive dynamic test data set is also available in [19].

A limitation of this study was the lack of consideration of acceleration-sensitive non-structural components. While the drift response of the structure supports fast return to function after a seismic event, the acceleration demands, which are heightened by the contributions of higher modes, could cause significant damage. Future work includes: (1) definition of target acceleration limits for the SLE, DE, and MCE_R informed by non-structural component criteria and (2) evaluation of the effect of heightened acceleration demands on expected loss for the building.

6 – ACKNOWLEDGMENTS

This project was supported by the National Science Foundation (NSF) NHERI Converging Design project under awards #2120683, #2120692, and #2120684. Special thanks to the prior NHERI TallWood team, supported by the NSF awards #1636164, #1634204, #1635363, #1635156, and #1634628. The authors wish to express their appreciation for the generous support and donations provided by our industry partners. For a full list of sponsors and collaborators refer to https://tallwoodinstitute.org/nheri-converging-design/. and http://nheritallwood.mines.edu/. The findings, opinions, recommendations, and conclusions in this paper are those of the authors and do not necessarily reflect the views of others, including the sponsors.

8 – REFERENCES

[1] Granello, G., Palermo, A., Pampanin, S., Pei, S., & van de Lindt, J. (2020). "Pres-Lam Buildings: State-of-the-Art." Journal of Structural Engineering, 146(6), 04020085. https://doi.org/10.1061/(ASCE)ST.1943-541X.0002603

[2] Abed, J., Rayburg, S., Rodwell, J., & Neave, M. (2022). "A Review of the Performance and Benefits of Mass Timber as an Alternative to Concrete and Steel for Improving the Sustainability of Structures." Sustainability, 14(9), 5570. https://doi.org/10.3390/su14095570

[3] Kontra, S., Barbosa, A. R., Sinha, A., Mishra, P., McBain, M., Pei, S., van de Lindt, J. W., & Simpson, B. G. (2025). "Whole-Building Life-Cycle Assessment in the Built Environment: A Ten- and Six-Story Shake-Table Test Building Case Study." Forest Products Journal, 75(1), 52–61. https://doi.org/10.13073/FPJ-D-24-00030R1

[4] Mar, D. (2010). "Design Examples using Mode Shaping Spines for Frame and Wall Buildings." In Proceedings of the 9th U.S. National and 10th Canadian Conference on Earthquake Engineering.

[5] Palermo, A., Pampanin, S., & Buchanan, A. (2006). "Experimental Investigations on LVL Seismic Resistant Wall and Frame Subassemblies." In Proceedings of First European Conference on Earthquake Engineering and Seismology.

[6] Sarti, F., Palermo, A., & Pampanin, S. (2016). "Quasi-Static Cyclic Testing of Two-Thirds Scale Unbonded Posttensioned Rocking Dissipative Timber Walls." Journal of Structural Engineering, 142(4), E4015005. https://doi.org/10.1061/(ASCE)ST.1943-541X.0001291

[7] Iqbal, A., Smith, T., Pampanin, S., Fragiacomo, M., Palermo, A., & Buchanan, A. H. (2016). "Experimental Performance and Structural Analysis of Plywood-Coupled LVL Walls." Journal of Structural Engineering, 142(2), 04015123. https://doi.org/10.1061/(ASCE)ST.1943-541X.0001383

[8] Brown, J. R., Li, M., Palermo, A., Pampanin, S., & Sarti, F. (2021). "Experimental Testing of a Low-Damage Post-Tensioned C-Shaped CLT Core-Wall." Journal of Structural Engineering, 147(3), 04020357. https://doi.org/10.1061/(ASCE)ST.1943-541X.0002926

[9] Akbas, T., Sause, R., Ricles, J. M., Ganey, R., Berman, J., Loftus, S., Dolan, J. D., Pei, S., van de Lindt, J. W., & Blomgren, H.-E. (2017). "Analytical and Experimental Lateral-Load Response of Self-Centering Posttensioned CLT Walls." Journal of Structural Engineering, 143(6), 04017019. https://doi.org/10.1061/(ASCE)ST.1943-541X.0001733

[10] Ganey, R., Berman, J., Akbas, T., Loftus, S., Daniel Dolan, J., Sause, R., Ricles, J., Pei, S., Lindt, J. V. D., & Blomgren, H.-E. (2017). "Experimental Investigation of Self-Centering Cross-Laminated Timber Walls." Journal of Structural Engineering, 143(10), 04017135. https://doi.org/10.1061/(ASCE)ST.1943-541X.0001877

[11] Blomgren, H.-E., Pei, S., Jin, Z., Powers, J., Dolan, J. D., van de Lindt, J. W., Barbosa, A. R., & Huang, D. (2019). "Full-Scale Shake Table Testing of Cross-Laminated Timber Rocking Shear Walls with Replaceable Components." Journal of Structural Engineering, 145(10), 04019115. https://doi.org/10.1061/(ASCE)ST.1943-541X.0002388

[12] Pei, S., van de Lindt, J. W., Barbosa, A. R., Berman, J. W., McDonnell, E., Daniel Dolan, J., Blomgren, H.-E., Zimmerman, R. B., Huang, D., & Wichman, S. (2019). "Experimental Seismic Response of a Resilient 2-Story Mass-Timber Building with Post-Tensioned Rocking Walls." Journal of Structural Engineering, 145(11), 04019120. https://doi.org/10.1061/(ASCE)ST.1943-541X.0002382

[13] Amer, A., Sause, R., & Ricles, J. (2024). "Experimental Response and Damage of SC-CLT Shear Walls under Multidirectional Cyclic Lateral Loading." Journal of Structural Engineering, 150(2), 04023215. https://doi.org/10.1061/JSENDH.STENG-12576

[14] Pei, S., Ryan, K. L., Berman, J. W., van de Lindt, J. W., Pryor, S., Huang, D., Wichman, S., Busch, A., Roser, W., Wynn, S. L., Ji, Y., Hutchinson, T., Sorosh, S., Zimmerman, R. B., & Dolan, J. (2024). "Shake-Table Testing of a Full-Scale 10-Story Resilient Mass Timber Building." Journal of Structural Engineering, 150(12), 04024183. https://doi.org/10.1061/JSENDH.STENG-13752

[15] Zimmerman, R. B., Blomgren, H.-E., McCutcheon, J., & Sinha, A. (2020). "Catalyst - a Mass Timber Core Wall Building with High Ductility Hold-Downs in a Seismic Region." In Proceedings of World Conference on Timber Engineering, Santiago, Chile.

[16] Dong, W., Li, M., Lee, C.-L., MacRae, G., & Abu, A. (2020). "Experimental testing of full-scale glulam frames with buckling restrained braces." Engineering Structures, 222, 111081. https://doi.org/10.1016/j.engstruct.2020.111081

[17] Araújo R., Gustavo A. (2022). "Design, Experimental Testing, and Numerical Analysis of a Three-Story Mass Timber Building with a Pivoting Spine and Buckling-Restrained Energy Dissipators." Master's Thesis Oregon State University.

[18] Araújo R., G. A., Simpson, B. G., Barbosa, A. R., Pieroni, L., Ho, T. X., Orozco O., G. F., Miyamoto, B. T., & Sinha, A. (forthcoming). "Experimental and Numerical Simulation of a Three-Story Mass Timber

 https://doi.org/10.52202/080513-0300

Building with a Pivoting Wall and Buckling-Restrained Boundary Elements." Journal of Structural Engineering. https://doi.org/10.1061/JSENDH/STENG-13781

[19] Barbosa, A., B. Simpson, J. van de Lindt, A. Sinha, T. Field, M. McBain, P. Uarac, S. Kontra, P. Mishra, L. Gioiella, L. Pieroni, S. Pryor, B. Saxey (2025). "Shake table testing program for mass timber and hybrid resilient structures datasets for the NHERI Converging Design project", in Shake table testing program of 6-story mass timber and hybrid resilient structures (NHERI Converging Design project). DesignSafe-CI. https://doi.org/10.17603/ds2-rh8q-rn95

[20] Uarac P. P. A., Barbosa, A. R., Sinha, A., van de Lindt, J. W., Simpson, B. G. (202X). "Full-Scale Shake Table Testing of a Resilient Six-Story Mass Timber Building with Self-Centering Rocking Walls." To be submitted to Journal of Structural Engineering.

[21] Field, T., Barbosa, A.R., Pryor, S., Simpson, B., Uarac, P.P.A, Sinha, A., van de Lindt, J.W. (2025). Shake-Table Testing of a Full-Scale Six-story Resilient Mass Timber-Steel Hybrid Building. Submitted to Journal of Structural Engineering

[22] Busch, A. (2023). "Design and Construction of Tall Mass Timber Buildings with Resilient Post-Tensioned Mass Timber Rocking Walls" Ph.D. Thesis, Colorado School of Mines.

[23] Huang, D. (2023). Optimized Seismic Design and Dynamic Response Analysis of Mass Timber Rocking Wall Lateral System. Ph.D. Thesis, Colorado School of Mines.

[24] Pryor, S., Pei, S., van de Lindt, J., and Huang, D. (2024). "Seismically Resilient Connections for Mass Timber Buildings." In Proceedings of 18th World Conference on Earthquake Engineering, Milan, Italy.

[25] Ancheta, T. D., Darragh, R. B., Stewart, J. P., Seyhan, E., Silva, W. J., Chiou, B. S. J., Wooddell, K. E., Graves, R. W., Kottke, A. R., Boore, D. M., Kishida, T., & Donahue, J. L. (2014). "NGA-West2 database." Earthquake Spectra, 30(3), 989-1005.

[26] Bozorgnia, Y., et al. (2022). NGA-Subduction research program. Earthquake Spectra, 38(2), 783-798.

[27] Kontra, Steven. (2024) "Glued-in Rods for Mass Timber Shear Wall Panel Splicing: Design, Implementation, and Performance." Master's Thesis Oregon State University.

[28] Micozzi, F., Morici, M., Zona, A., & Dall'Asta, A. (2023). "Vision-Based Structural Monitoring: Application to a Medium-Span Post-Tensioned Concrete Bridge under Vehicular Traffic." INFRASTRUCTURES, 8(10), 152. https://doi.org/10.3390/infrastructures8100152

[29] Skolnik, D. A., & Wallace, J. W. (2010). "Critical assessment of interstory drift measurements." Journal of structural engineering, 136(12), 1574-1584.

[30] McCormick, J., Aburano, H., Ikenaga, M., & Nakashima, M. (2008). "Permissible residual deformation levels for building structures considering both safety and human elements." In Proceedings of the 14th World Conference on Earthquake Engineering, Beijing, China.

[31] Applied Technology Council, & National Earthquake Hazards Reduction Program (US). (2018). "Seismic Performance Assessment of Buildings, Volume 1—Methodology, Second Edition." Federal Emergency Management Agency.